RELATIONSHIP BETWEEN DEEP CHLOROPHYLL MAXIMUM AND SURFACE CHLOROPHYLL CONCENTRATION IN THE CALIFORNIA CURRENT SYSTEM

ROBERTO MILLÁN-NÚÑEZ
Facultad de Ciencias Marinas, UABC
P.O. Box 453
Ensenada, B.C.
México

SAÚL ALVAREZ-BORREGO
Departamento de Ecología, CICESE
P.O. Box 2732
Ensenada, B.C.
México

CHARLES C. TREES
Center for Hydro-Optics and Remote Sensing
San Diego State University
6505 Alvarado Rd. Suite 206
San Diego, California 92120

ABSTRACT

Empirical relationships were derived to estimate the depth (Z_m) and concentration (Chl_m) of the deep chlorophyll maximum (DCM) in the California Current System (CCS) between 28° and 37°N, using CalCOFI data (1978–92). Because primary productivity may be modeled from remotely sensed ocean color data, it is important to be able to predict Z_m and Chl_m. The DCM is a persistent feature of this system, with the average Z_m generally increasing from north to south, and with distance from shore. Meanwhile, Chl_m is higher inshore than offshore. During ENSO events, Z_m was deeper, and Chl_m was lower than during normal years. The studied area was spatially divided into six subregions, and temporally into warm and cool seasons. Regression models were developed for each subregion and season to estimate Z_m and Chl_m as functions of surface chlorophyll.

INTRODUCTION

Satellites provide the only observational platform by which total and new primary productivity can be monitored at ocean-basin scales (Platt and Sathyendranath 1988; Sathyendranath et al. 1991). Unfortunately, remotely sensed ocean color is limited to depth at which 90% of the backscattered irradiance from the water column originates. Remote sensors provide information on the average photosynthetic pigment concentration for the upper 22% of the euphotic zone (Kirk 1983).

Empirical and semianalytical algorithms to estimate primary productivity from satellite-derived photosynthetic pigments have been compared (Balch et al. 1989, 1992; Platt and Sathyendranath 1993). These productivity models apply to the entire euphotic zone; ideally, they should use the vertical profile of pigment biomass as input. Therefore a gap exists between the limited satellite pigment information and what is needed for modeling. The assumption of a mixed layer with a homogeneous pigment distribution could lead to an over- or underestimation of productivity, depending on the shape of the biomass distribution (Platt et al. 1988, 1991).

A common characteristic of the California Current System (CCS) is the presence of a deep chlorophyll maximum (DCM) (Cullen and Eppley 1981; Hayward et al.

1995). This maximum changes in depth and concentration from inshore to offshore (Hayward et al. 1995). A DCM deeper than the 1% light level may contribute as much as 10% of the total integrated primary productivity (Venrick et al. 1973).

Since the early studies on the DCM (Riley 1949), a large effort has been directed to understanding such features (Varela et al. 1992, and others cited therein). In our study area, the DCM coincides with the upper part of the nitracline, where nitrate concentration is about 1.0 µM (Hayward et al. 1995).

The purpose of our work is to provide empirical algorithms to estimate the DCM concentration (Chl_m) and depth (Z_m) as a function of surface properties that may be estimated with data generated by remote sensors, such as surface chlorophyll concentration (Chl_s) and T °C. The underlying assumption is that for a given area of the CCS, in a given season, the relationships between the surface chlorophyll concentration and Chl_m, and Z_m, are constant or at least predictable.

DATA AND METHODS

All observations fall within the region bounded by CalCOFI line 60 on the north, line 120 on the south, and stations XX.110 on the west (figure 1). We used the CalCOFI database for the 1978–92 period. Chlorophyll *a* concentrations were determined by the standard fluorometric method (Yentsch and Menzel 1963; Holm-Hansen et al. 1965).

Initially, our data base had 4,160 chlorophyll profiles. We discarded 18% of these profiles because they presented two or more maxima. We tabulated the DCM concentration and depth, as well as the surface temperature and surface chlorophyll concentration for each of the remaining 3,410 profiles. Table 1 shows the number of useful profiles available for each year, month, and area.

The study area was divided into three regions following Lynn and Simpson (1987): Central California (CC), Southern California (SC), and Baja California (BC; figure 1). We then plotted Z_m versus distance from shore for each CalCOFI line, and we divided the regions into inshore (i) and offshore (o) subregions (figure 1) according to the behavior of Z_m (figure 2 illustrates examples). These inshore-offshore subregions
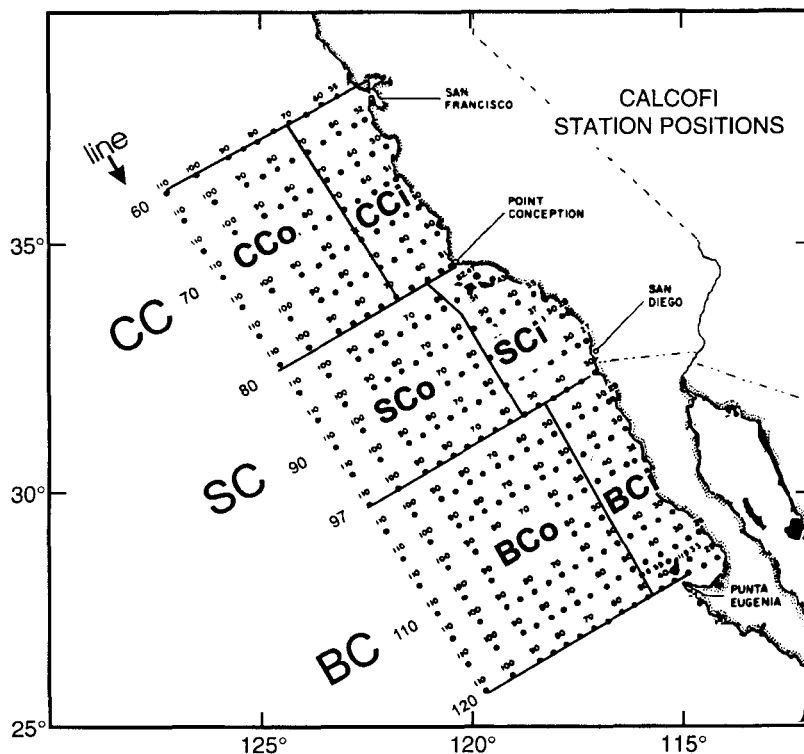
Figure 1.   Study area: Central California (CC); Southern California (SC); and Baja California (BC) regions; inshore (i) and offshore (o) subregions.

TABLE 1
Numbers of Chlorophyll Profiles Used for Each Year, Month, and Season for Each Subregion

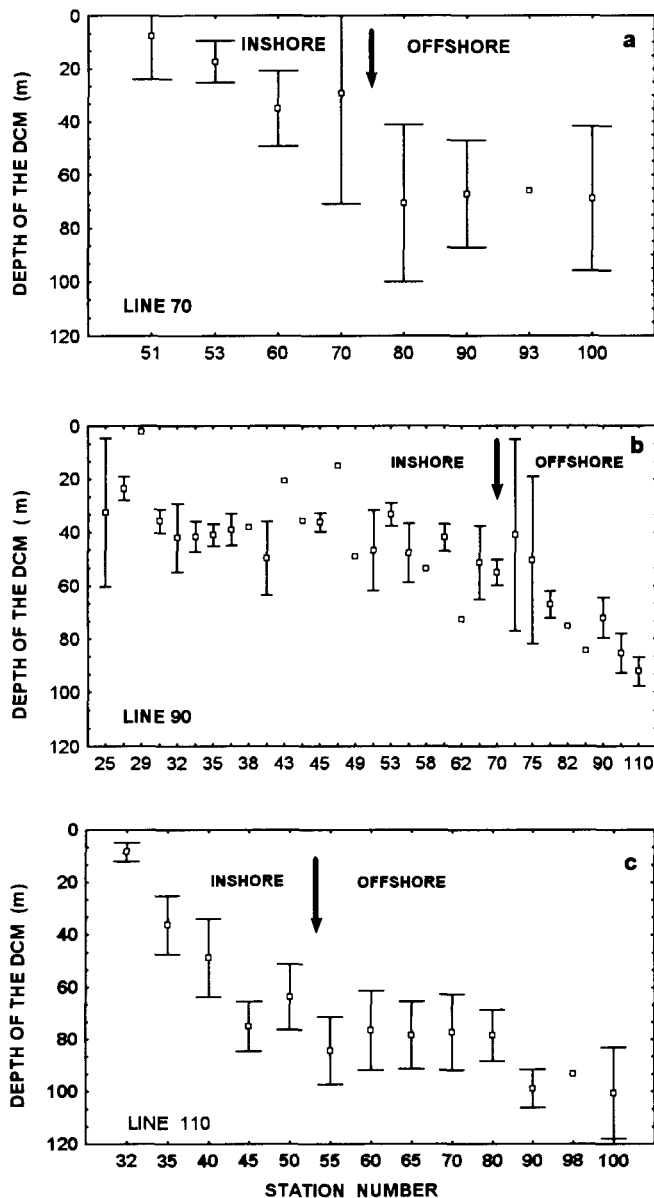|	CCi	CCo	SCi	SCo	BCi	BCo	Total
Year							
1978	51	49	83	109	93	113	498
1981	1	0	19	26	6	11	63
1983	0	0	70	23	0	0	93
1984	33	65	230	231	98	162	819
1985	12	12	103	89	0	0	216
1986	12	15	113	94	0	0	234
1987	9	10	117	112	0	0	248
1988	23	11	123	99	1	0	257
1989	16	16	112	120	0	0	264
1990	12	10	100	105	0	0	227
1991	13	14	107	108	0	0	242
1992	11	17	100	121	0	0	249
Month							
January	16	25	130	124	43	37	375
February	19	24	93	113	15	27	291
March	18	20	126	94	25	24	307
April	12	16	149	146	25	35	383
May	20	0	143	129	0	0	292
June	0	0	51	35	34	70	190
July	24	44	136	137	22	45	408
August	32	36	112	127	18	27	352
September	9	7	77	70	1	0	164
October	28	29	112	119	9	6	303
November	15	18	141	135	6	15	330
December	0	0	7	8	0	0	15
Season							
Cool	85	85	641	606	142	194	1,753
Warm	108	134	636	631	56	92	1,657
Total	193	219	1,227	1,237	198	286	3,410

Figure 2.   Depth of DCM at each station of CalCOFI lines: a, 70; b, 90; and c, 110. Arrows indicate the limit between inshore and offshore subregions.

TABLE 2
Surface Chlorophyll Concentration Interval
for Each Category

Category	Concentration $(mg \cdot m^{-3})$
1	≤ 0.1 $mg \cdot m^{-3}$
2	>0.1 y ≤ 0.2 $mg \cdot m^{-3}$
3	>0.2 y ≤ 0.5 $mg \cdot m^{-3}$
4	>0.5 y ≤ 1.0 $mg \cdot m^{-3}$
5	>1.0 y ≤ 2.0 $mg \cdot m^{-3}$
6	>2.0 y ≤ 5.0 $mg \cdot m^{-3}$
7	>5.0 $mg \cdot m^{-3}$

thus we grouped them into a single category. Within region BC, categories 4 and 6 presented the same Z_m, but they were kept separate.

We built regression models of the means of Chl_m and Z_m for each subregion, season, and category, as functions of the Chl_s mean for each category.

RESULTS AND DISCUSSION

Within the CC region the mean Z_m increased from less than 10 m at station 51 to about 70 m at station 80, and then it remained nearly constant with greater distance from shore (figure 2a). The behavior of Z_m within region SC was different compared to that of regions CC and BC. In this middle region, it changed between 20 and 50 m, from nearshore to station 65, without a particular pattern, and then increased to 95 m at station 110 (figure 2b). The behavior of the mean Z_m within region BC was similar to that in region CC, but the inflection point was closer to shore (station 50, figure 2c). Cullen and Eppley (1981) observed the increase of Z_m with distance offshore.

The mean Chl_s values for the whole year tended to be lower during the 1983, 1987, and 1992 ENSO events than during the other years (figure 4). Also, their 95% confidence intervals tended to be shorter during the ENSO years. The mean of Chl_m showed a similar behavior. The mean Z_m also tended to be larger for ENSO years (not illustrated). Typically, the oceanic effects of ENSO events in the CCS include a strong and broad countercurrent/undercurrent along the continental margin, anomalous poleward winds along the coast, and a depressed thermocline and nutricline, ultimately causing a strong effect on the marine biota (Lynn et al. 1995, and others cited therein). Our Chl_s time series is too short to show a clear interannual tendency (figure 4). Nevertheless, there is some indication of a Chl_s tendency to decrease, resembling the general zooplankton decrease described by Roemmich and McGowan (1995) for the period 1951–93.

The monthly Chl_s means for all regions show the typical seasonal variation in temperate waters, with maxima at the end of winter and spring (figure 5). The average year of Chl_m, for each subregion, generally shows
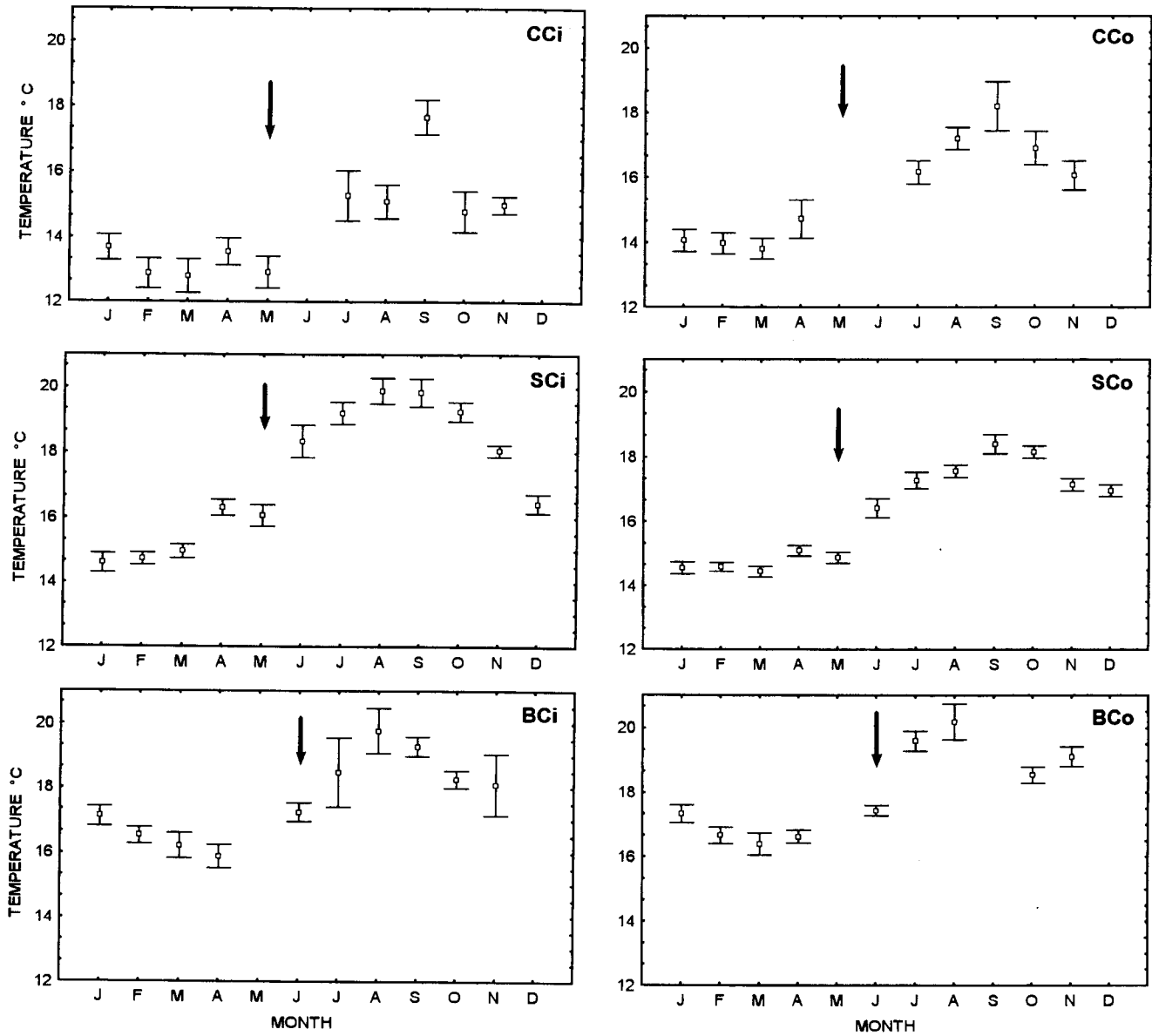
coincide very closely with those proposed by Lynn and Simpson (1987) based on sigma-t analysis.

We used the 95% range estimate of the surface temperature monthly mean for the whole 1978–92 period, for each subregion, to define seasons (figure 3). The cool season was January through May for CC and SC regions, January through June for the BC region. The rest of the year is considered the warm season.

Surface chlorophyll values were grouped into seven categories (table 2). The criterion for defining these seven categories was that Z_m had to be significantly different at each category, at the 95% confidence level. Categories 4 and 5 had the same Z_m within region CC,

Figure 3.   Monthly mean surface T °C for each subregion, and for the whole study period. *Bars* are the 95% confidence intervals. *Arrows* indicate the end of the cool season.
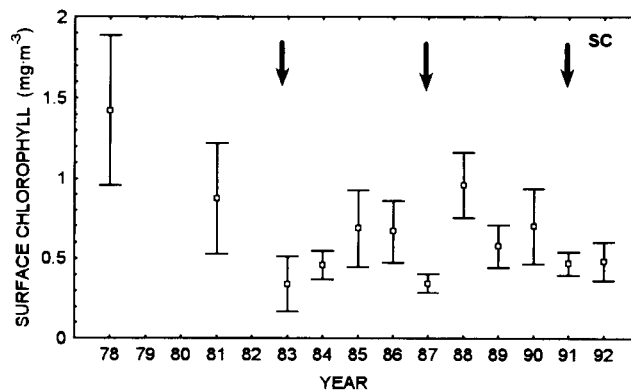

Figure 4.   Mean surface chlorophyll for each year for the Southern California region. *Bars* are the 95% confidence intervals. *Arrows* indicate ENSO events.
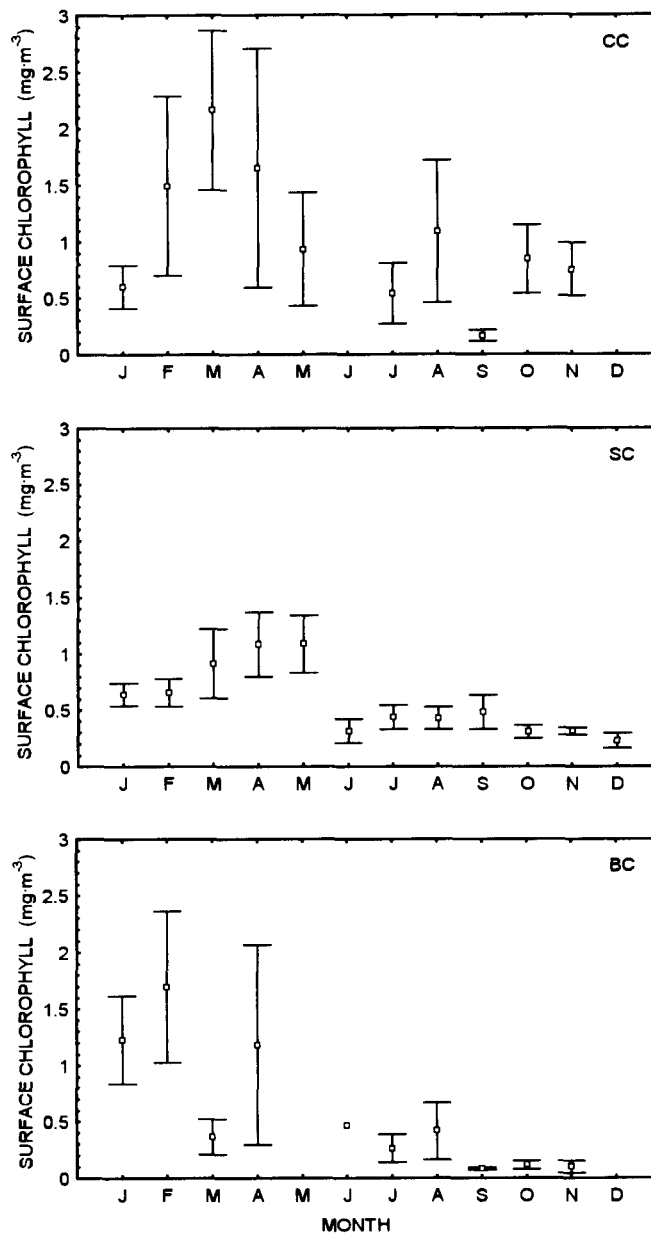
Figure 5.   Monthly mean surface chlorophyll for the whole study period, and for each region. *Bars* are the 95% confidence intervals.

a seasonal variation with a spring maximum (figure 6). The maximum mean Chl_m was highest for CCi (7 mg m^{-3}), and it was lowest for SCo and BCo (2.3 mg m^{-3}).

There is no general behavior of the Z_m seasonal variation (figure 7). Within CCi and CCo, Z_m showed lowest values during fall and winter, and maximum values during spring and summer. However, Z_m was largest during summer and fall for SCi, and from the end of spring through December for SCo. Meanwhile, Z_m had minimum values at the beginning of winter and end of summer, and large values during the rest of the year, within BCi and BCo.

The overall mean surface chlorophyll concentration ($MChl_s$) for cool and warm periods was greater for inshore than for offshore subregions (figure 8a, b). The $MChl_s$ was significantly greater for CCi than for SCi and BCi. There was no significant $MChl_s$ difference for the offshore subregions at the 95% confidence level, with the exception of BCo during the warm season, which was lower than the other two (figure 8a, b).

In general, the behavior of the overall mean Chl_m ($MChl_m$) for all cool and warm periods was similar to that of $MChl_s$ (figure 8 a–d). The $MChl_m$ was higher for inshore than for offshore subregions (figure 8c, d).
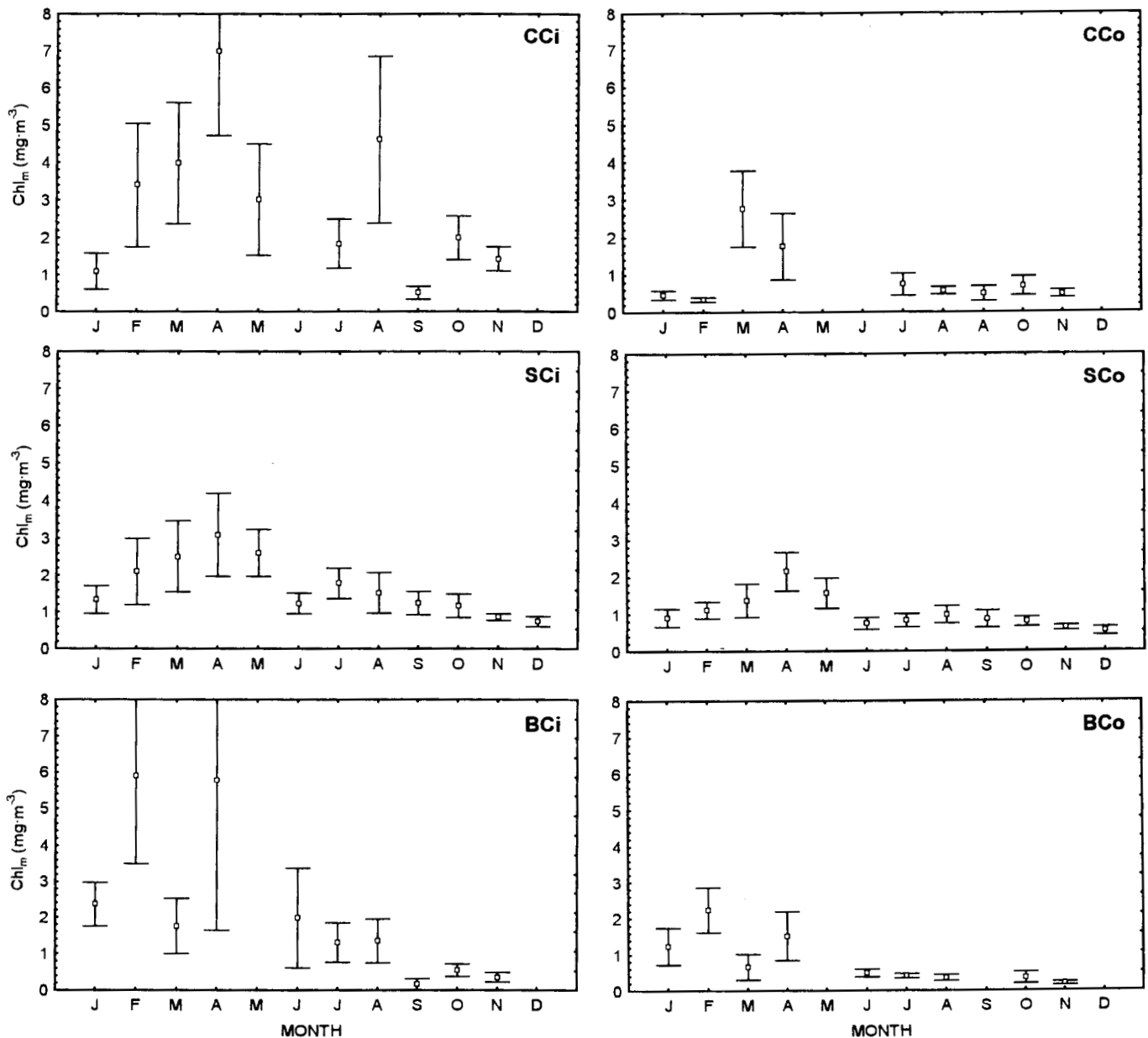
245

Figure 6. Monthly mean chlorophyll concentration at the DCM for each subregion. *Bars* are the 95% confidence intervals.

During the cool season, there is no significant variation of $MChl_m$ in the north-south direction (figure 8c). Nevertheless, during the warm season there was a significant decrease of $MChl_m$ from north to south (figure 8d). The overall mean of Z_m (MZ_m) showed a difference of 30–40 m between inshore and offshore subregions, with larger values for the latter (figure 8e, f). The MZ_m generally increased from north to south.

The $MChl_m/MChl_s$ ratio increased both from inshore to offshore and from north to south during the cool season (not illustrated). The largest difference for this season was 1.7 for CCi to 4.5 for BCo. During the

warm season, the $MChl_m/MChl_s$ ratio did not follow a general trend; it increased from inshore to offshore only in the CC and BC regions (from 3.0 to 4.2); in the SC region there was no significant difference. Also, during the warm season there was no significant change of the $MChl_m/MChl_s$ ratio from north to south in the whole study area (not illustrated).

We calculated the mean of all Chl_m and the mean of all Z_m for each subregion and season and for each surface-chlorophyll concentration category ($CMChl_m$ and CMZ_m), as well as the mean of all Chl_s values within each category ($CMChl_s$; table 3). In some cases, graphs
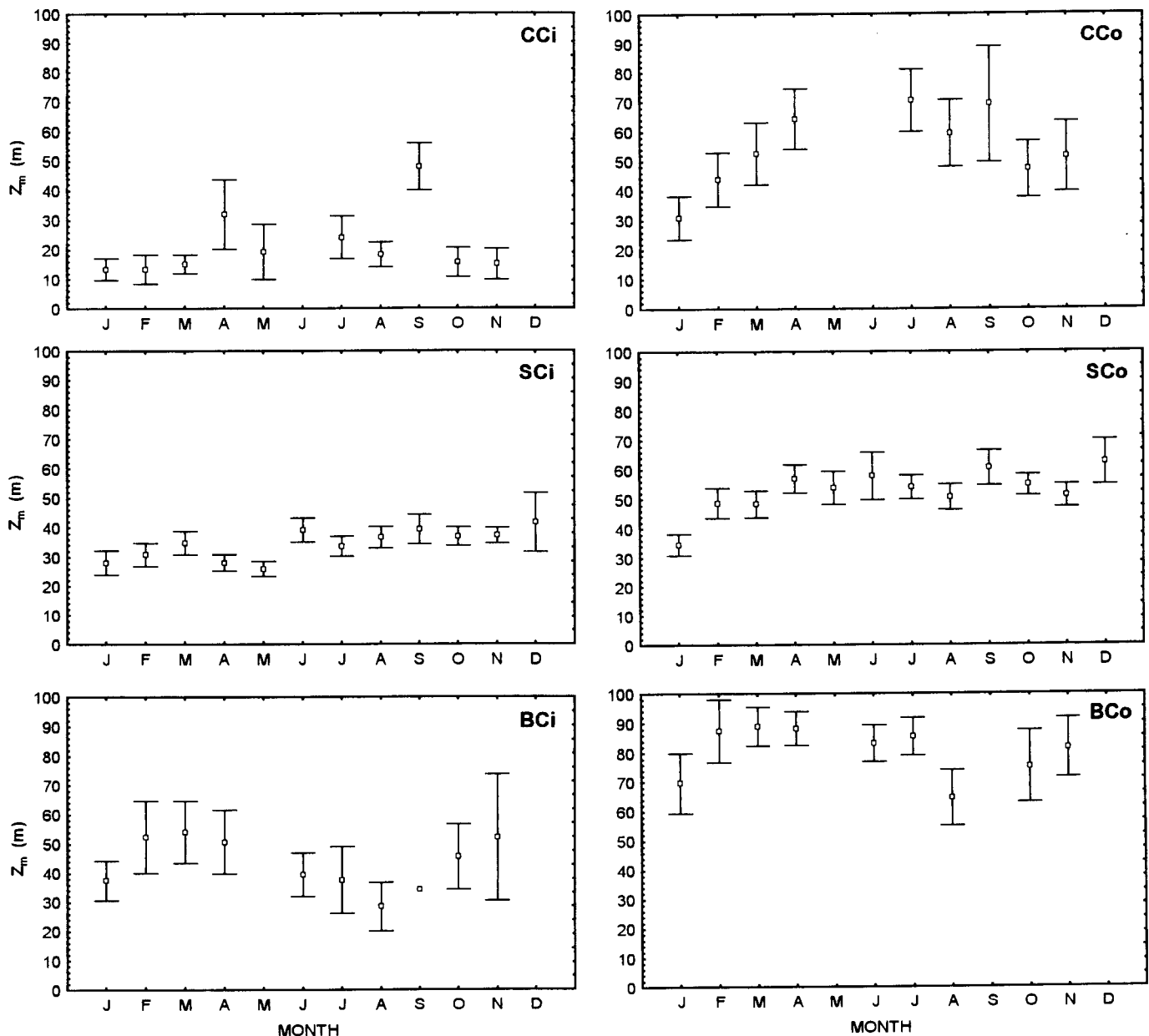
Figure 7. Monthly mean DCM depth (Z_m) for each subregion. *Bars* are the 95% confidence intervals.

of $CMChl_m$ versus $CMChl_s$ suggest a positive exponential relationship, and in other cases they show a linear relationship (not illustrated). Something similar is shown by the mean of all Z_m's for each subregion and season (CMZ_m), but it was either an exponential or linear decrease, instead of an increase (not illustrated).

We built simple linear regression models of $CMChl_m$, or $\ln CMChl_m$, as functions of either $CMChl_s$ or $\ln CMChl_s$, and we did the same for CMZ_m. Adding surface T °C to the models as one more independent variable did not contribute significantly to the improvement

of the correlation coefficient (r) at the 95% confidence level.

Thereafter, we chose the models with the largest r for each subregion and season (table 4). All chosen regression models have r greater than 0.90, except for the CMZ_m models for the cool season of CCo and BCo, and the CMZ_m model for the warm season of CCi. The regression models for the warm season of BCo are strongly limited by the fact that we only had data for chlorophyll categories one, two, and three. Nevertheless, these three points fell close to the straight line ($r > 0.99$).
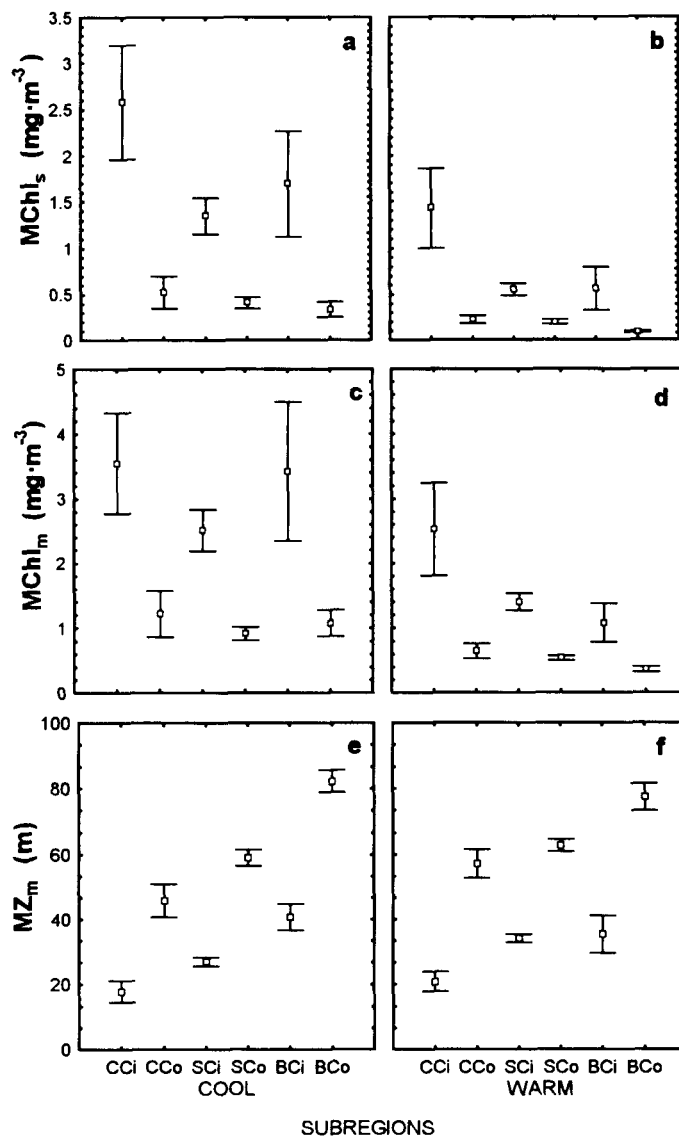
Figure 8. Overall mean for each subregion and season: *a* and *b*, surface chlorophyll concentration; *c* and *d*, chlorophyll concentration at the DCM; *e* and *f*, DCM depth. *Bars* are the 95% confidence intervals.

In most cases, our regression models explain up to 98% of the total sums of squares of $CMChl_m$ and CMZ_m (table 4). Using data from off Southwest Africa, Baja California, and Peru, Lorenzen (1970) found a high linear relationship between ln Chl_s and the logarithm of the integrated Chl for the whole euphotic zone ($r = 0.90$). Hayward and Venrick (1982) also found Chl_s correlated with integrated chlorophyll ($r = 0.86$) in the CCS. However, the latter authors reported a lack of correlation of surface and integrated chlorophyll in the central North Pacific. It is necessary to analyze available data from the central North Pacific to study a possible correlation of $CMChl_s$ with $CMChl_m$ and CMZ_m.

Our algorithms are not capable of predicting the instantaneous Chl_m and Z_m for a particular geographic location. In other words, when our algorithms are applied to estimate $CMChl_m$ and CMZ_m, these predicted values should be used for the whole area with all the Chl_s values within the respective chlorophyll category, within the corresponding subregion, and for the whole season.

ACKNOWLEDGMENTS

TABLE 3
Means of Chl_s, Chl_m, and Z_m for Each Subregion, Season, and Category

Subregion	Category	Cool season				Warm season			
		$CMChl_s$	$CMChl_m$	CMZ_m	n	$CMChl_s$	$CMChl_m$	CMZ_m	n
CCi	1	0.07	0.41	69.8	2	0.08	1.39	10.9	2
	2	0.10	0.34	31.6	1	0.14	0.63	47.6	10
	3	0.28	0.52	28.5	6	0.30	0.91	32.1	30
	4	0.99	1.70	16.7	46	1.09	2.73	14.8	49
	6	3.49	5.44	16.7	17	3.06	3.92	9.6	12
	7	7.75	8.95	11.8	13	9.07	9.95	5.1	5
CCo	1	0.07	0.77	75.6	12	0.06	0.38	79.6	41
	2	0.13	0.36	54.5	22	0.13	0.57	60.5	48
	3	0.32	0.50	28.5	26	0.29	0.76	40.5	30
	4	0.98	2.43	43.4	22	0.72	0.87	17.5	14
	6	2.48	6.45	43.1	2	2.27	2.33	8.3	1
	7	6.24	6.81	14.0	1				
SCi	1	0.89	0.71	49.0	10	0.80	0.67	52.3	17
	2	0.15	0.79	48.7	118	0.14	0.82	48.6	202
	3	0.31	1.34	32.5	176	0.29	1.17	34.1	253
	4	0.71	1.27	18.2	124	0.72	1.73	18.2	83
	5	1.39	2.61	16.0	111	1.37	2.41	12.0	47
	6	3.01	5.11	14.0	63	3.27	4.26	8.7	31
	7	9.25	13.01	10.8	39	7.33	8.85	11.0	3
SCo	1	0.72	0.44	90.4	163	0.75	0.34	82.7	229
	2	0.13	0.49	65.4	191	0.13	0.52	62.1	259
	3	0.33	0.59	36.6	109	0.29	0.69	38.4	104
	4	0.68	1.43	36.4	87	0.70	0.83	17.2	23
	5	1.42	2.95	30.6	37	1.33	1.78	12.6	12
	6	2.58	3.92	14.2	16	3.05	3.37	9.8	4
	7	8.34	10.04	15.8	3				
BCi	1	0.82	0.67	68.9	17	0.85	0.29	71.7	4
	2	0.14	0.75	60.7	42	0.13	0.47	48.4	25
	3	0.27	1.19	35.9	14	0.31	1.38	31.5	11
	4	0.72	1.48	18.9	11	0.67	0.93	12.1	6
	5	1.43	3.38	28.6	26	1.28	1.72	11.6	6
	6	3.06	6.53	23.3	19	2.67	4.01	9.4	3
	7	9.75	15.23	11.5	13	5.17	5.17	0.0	1
BCo	1	0.07	0.38	93.0	97	0.06	0.29	84.7	60
	2	0.12	0.45	78.3	52	0.11	0.45	67.4	27
	3	0.29	0.94	60.1	5	0.27	0.62	39.1	5
	4	0.73	3.02	78.3	22				
	5	1.35	4.68	67.8	9				
	6	2.57	3.73	25.4	9				
	7								

TABLE 4
Regression Equations to Estimate $CMChl_m$ and CMZ_m as Functions of $CMChl_s$, for Each Subregion and Season

Province	n	Cool season	r	n	Warm season	r
CCi	7	$CMChl_m = 0.4603 + 1.1511 (Chl_s)$ $\ln CMZ_m = 3.0480 - 0.3022 (\ln Chl_s)$	0.99 -0.91	7	$CMChl_m = 0.9855 + 0.9914 (Chl_s)$ $\ln CMZ_m = 3.1286 - 0.1775 (Chl_s)$	0.99 -0.76
CCo	7	$CMChl_m = 3.7055 + 1.5930 (\ln Chl_s)$ $\ln CMZ_m = 3.9875 - 0.2023 (Chl_s)$	0.92 -0.82	6	$\ln CMChl_m = 0.2956 + 0.4713 (\ln Chl_s)$ $\ln CMZ_m = 2.6991 - 0.6469 (\ln Chl_s)$	0.96 -0.99
SCi	7	$CMChl_m = 0.6877 + 1.3436 (Chl_s)$ $\ln CMZ_m = 3.0280 - 0.3576 (\ln Chl_s)$	0.99 -0.97	7	$CMChl_m = 0.7666 + 1.1021 (Chl_s)$ $\ln CMZ_m = 2.8954 - 0.4274 (\ln Chl_s)$	0.99 -0.95
SCo	7	$CMChl_m = 0.5959 + 1.1577 (Chl_s)$ $\ln CMZ_m = 3.3829 - 0.3836 (\ln Chl_s)$	0.99 -0.95	6	$CMChl_m = 0.3273 + 1.0018 (Chl_s)$ $\ln CMZ_m = 2.8177 - 0.6168 (\ln Chl_s)$	0.99 -0.98
BCi	7	$CMChl_m = 0.8380 + 1.5113 (Chl_s)$ $\ln CMZ_m = 3.2888 - 0.3410 (\ln Chl_s)$	0.99 -0.92	7	$CMChl_m = 0.5707 + 0.9679 (Chl_s)$ $\ln CMZ_m = 3.7434 - 0.7169 (Chl_s)$	0.96 -0.94
BCo	6	$\ln CMChl_m = 1.0013 + 0.7648 (\ln Chl_s)$ $\ln CMZ_m = 4.4986 - 0.4244 (Chl_s)$	0.96 -0.88	3	$CMChl_m = 0.9235 + 0.2277 (\ln Chl_s)$ $CMZ_m = -2.3330 - 32.24 (\ln Chl_s)$	0.99 -0.99

LITERATURE CITED

Balch, W. M., M. R. Abbott, and R. W. Eppley. 1989. Remote sensing of primary production. I. A comparison of empirical and semi-analytical algorithms. Deep-Sea Res. 36(2):281–295.

Balch, W. M., R. Evans, J. Brown, G. Feldman, C. R. McClain, and W. Esaias. 1992. The remote sensing of ocean primary productivity: use of new data compilation to test satellite algorithms. J. Geophys. Res. 99:2279–2293.

Cullen, J. J., and R. W. Eppley. 1981. Chlorophyll maximum layers of the Southern California Bight and possible mechanisms of their formation and maintenance. Oceanol. Acta 4:23–32.

Hayward, T. L., and E. L. Venrick. 1982. Relation between surface chlorophyll, integrated chlorophyll, and primary production. Mar. Biol. 69:247–252.

Hayward, T. L., D. R. Cayan, P. J. S. Franks, R. J. Lynn, A. W. Mantyla, J. A. McGowan, P. E. Smith, F. B. Schwing, and E. L. Venrick. 1995. The state of the California Current in 1994–1995. Calif. Coop. Oceanic Fish. Invest. Rep. 35:19–35.

Holm-Hansen, O., C. Lorenzen, R. W. Holmes, and J. D. H. Strickland. 1965. Fluorometric determination of chlorophyll. J. Cons. Perm. Int. Explor. Mer 30:3–15.

Kirk, J. T. O. 1983. Light and photosynthesis in aquatic ecosystems. Cambridge Univ. Press, Cambridge, 401 pp.

Lorenzen, C. J. 1970. Surface chlorophyll as an index of the depth, chlorophyll content, and primary productivity of the euphotic layer. Limnol. Oceanogr. 15:479–480.

Lynn, R. J., and J. J. Simpson. 1987. The California Current System: the seasonal variability of its physical characteristics. J. Geophys. Res. 92:12,947–12,966.

Lynn, R. J., F. B. Schwing, and T. L. Hayward. 1995. The effect of the 1991–1993 ENSO on the California Current System. Calif. Coop. Oceanic Fish. Invest. Rep. 36:19–39.

Platt, T., and S. Sathyendranath. 1988. Oceanic primary production: estimation by remote sensing at local and regional scales. Science 241:1,613–1,620.

———. 1993. Estimators of primary production for interpretation of remotely sensed data on ocean color. J. Geophys. Res. 98:14,561–14,576.

Platt, T., S. Sathyendranath, C. M. Caverhill, and M. R. Lewis. 1988. Ocean primary production and available light: further algorithms for remote sensing. Deep-Sea Res. 35:855–879.

Platt, T., C. Caverhill, and S. Sathyendranath. 1991. Basin-scale estimates of oceanic primary production by remote sensing: the North Atlantic. J. Geophys. Res. 96:15,147–15,159.

Riley, G. A. 1949. Quantitative ecology of the plankton of the western North Atlantic. Bull. Bingham Oceanogr. Collect. 12:1–169.

Roemmich, D., and J. McGowan. 1995. Climatic warming and the decline of zooplankton in the California Current. Science 267:1324–1326.

Sathyendranath, S., T. Platt, E. P. W. Horne, W. G. Harrison, O. Ulloa, R. Outerbridge, and N. Hoepffner. 1991. Estimation of new production in the ocean by compound remote sensing. Nature 353:129–133.

Varela, R. A., A. Cruzado, J. Tintoré, and E. Garcia Landona. 1992. Modeling the deep-chlorophyll maximum: a coupled physical-biological approach. J. Mar. Res. 50:441–463.

Venrick, E. L., J. A. McGowan, and A. W. Mantyla. 1973. Deep maxima of photosynthetic chlorophyll in the Pacific Ocean. Fish. Bull., U.S. 71:41–52.

Yentsch, C. S., and D. W. Menzel. 1963. A method for the determination of phytoplankton, chlorophyll and phaeophytin by fluorescence. Deep-Sea Res. 10:221–231.